# Ion Cyclotron Antenna Impurity Production and Real Time Matching in Alcator C-Mod

S.J. Wukitch, , Y. Lin, B. LaBombard, B. Lipschultz, D. Whyte, and the Alcator C-Mod Team

MIT Plasma Science and Fusion Center, Cambridge MA 02139 USA

Email: wukitch@psfc.mit.edu

**Abstract.** In C-Mod, high performance plasmas require impurity control and injection of efficient, reliable ion cyclotron range of frequency (ICRF) power. To control Mo impurities boronization is frequently applied where the lifetime is proportional to number of RF joules injected. The erosion rate of boron films by ICRF-derived processes is estimated to be 15-20 nm/s. Assuming a similar net erosion rate for beryllium in ITER, the 1 cm beryllium thick armor could be eroded in ~1000 discharges (400 second discharges), a shortened lifetime. Emissive probe measurements of the local plasma potential at the plasma limiter confirm the presence of an enhanced plasma voltage when ICRF power is applied and the probe is magnetically linked to an active antenna. Measurements showed that the plasma potential voltage scaled with the square root of the RF power for L-mode, was enhanced in H-mode, and was present with both insulating and conducting limiter tiles. While the L-mode power dependence was expected, the increase in plasma potentials voltages with H-mode was significantly larger than expected. For the insulating tiles case, the enhanced potentials were expected to be eliminated. To transfer power to the plasma throughout a discharge, we have deployed a real-time matching system to minimize the VSWR. This system consists of two fast ferrite tuners (FFT) arranged in a triple stub configuration. We have demonstrated FFT usage at high power (1.85 MW coupled) while low VSWR was maintained over a wide range of plasma conditions. Furthermore, operation with ELMs shows that system matching was maintained throughout the ELM with tolerable reflection coefficient.

## 1.0 Introduction

Ion cyclotron range of frequency (ICRF) power is envisioned to be one of the principle auxiliary heating actuators for ITER and future fusion reactors.[1] To inject ICRF power, the coupling antenna structure needs to be situated near the plasma edge and the antenna input impedance needs to be transformed to match the output impedance of the transmitter. One of the primary ICRF utilization challenges is to reduce/eliminate specific ICRF impurity production resulting from the close proximity of the coupling structure and the plasma. Another challenge is to maintain and follow the antenna input impedance over a wide range of plasma conditions for reliable and efficient power transfer.

In next step devices including ITER, high-Z metallic plasma facing components (PFCs) are being considered despite obvious obstacles.[2] Particularly in a tokamak with metallic PFCs, controlling impurity production associated with ICRF is critical to its utilization. Ample evidence from C-Mod and other devices indicates that the ICRF is enhancing the sheath potential. A generally accepted model for ICRF induced impurity production is enhanced sputtering caused by RF rectified sheaths (RF sheaths) with substantially higher sheath voltages than expected for thermal sheaths (~3-4Te).[3] Previously a prescription to ameliorate impurity production was developed empirically for experiments with carbon PFCs.[4]

A generic ICRF matching network transforms the largely reactive antenna impedance and ideally would maintain this match despite the plasma induced variations which can have fast (<100 μsec) times scales.[5] A mismatch can reduce the maximum power output available from a generator, and can also unnecessarily force the generator to shut off because an arc

and load variation can not always be distinguished. Therefore, a matching network that is intolerant to or follows the antenna load variation in real-time would maximize the generator power, raise the RF power utilization, and improve experimental flexibility.

Despite the differences in geometric size between ITER (R=6.2m) and Alcator C-Mod (R=0.67 m), C-Mod has characteristics that are similar to conditions expected in ITER. The C-Mod ICRF antennas can obtain power densities (10 $MW/m^2$) in excess of the ITER antennas. The RF wave single-pass absorption is similar; thus, the RF fields in C-Mod plasmas will be localized toroidally. Furthermore, C-Mod utilizes high-Z (molybdenum) PFCs. The scrape off layer is also opaque to neutrals in C-Mod, an important consideration for impurity transport, as it is expected in ITER. In addition, beryllium has been proposed to cover most of the first wall and the ICRF faraday screen in ITER. In C-Mod, we can coat the PFCs with a low-Z boron film in-situ, using the so-called 'boronization' technique allowing an opportunity to investigate the compatibility of high power ICRF and low-Z films. C-Mod also affords access to a wide variety of plasma conditions including edge localized modes (ELMs) and H-mode plasmas providing an opportunity to test load tolerant/real time matching networks. In the following, we present estimates of the boron erosion rate and measurements of plasma potential modifications associated with the ICRF under a variety of plasma conditions. We also present the results from experiments utilizing a matching network based on a fast ferrite tuner (FFT).

Alcator C-Mod is a compact (major radius R = 0.67 m, minor radius a = 0.22 m), high field ($B_T \leq 8.1$ T) diverted tokamak[6]. The discharges analyzed here are lower single null D(H) (minority in parentheses) ICRF heated discharges. Although a range of toroidal fields and plasmas currents were investigated, the majority of the data was obtained for discharges with the on-axis toroidal field, $B_T$, was 5.4 T, and the plasma current, $I_p$, was 1 MA. The ICRF heating power is coupled to the plasma via three fast wave antennas. The two-strap antennas, D and E,[7] are operated in dipole $(0,\pi)$ phasing, at 80.5 and 80 MHz, respectively and the four-strap antenna, J,[8] is operated at 78 MHz in dipole phase $(0,\pi,0,\pi)$. Utilizing an electron cyclotron resonance discharge (ECDC), a thin film of boron is deposited on the PFCs, so-called boronization, with the boronization plasma characteristics have been reported elsewhere.[9] Boron deposition is limited to the radial region where the boronization plasma density is significant, a region is bounded by the cyclotron resonance on the inboard side and the upper hybrid resonance on the outboard where the radial separation between the two resonances is typically ~7-8 cm. For the experiments described herein, a thin film (15-20 nm) is applied by sweeping the ECDC resonance location between 0.65 m and 0.75 m for 10 minutes.

## 2.0 Boron Film Erosion

To ameliorate ICRF impurity production, coating the tokamak with low Z material, beryllium for example, has been effective for experiments with carbon PFCs. As noted above, beryllium has been proposed to cover ITER PFCs, including the ICRF Faraday screen. In C-Mod, the boron film erosion and the RF sheaths were linked to the active antenna in previous experiments.[10, 11] Utilizing between discharge boronization to apply a thin film, the erosion rate of low Z materials by RF sheaths can be estimated by observing when impurity control is lost during an H-mode. As an example, Figure 1 shows progressive loss of impurity control following a single application of boron film. We conclude that the boron film is effectively removed in a single discharge using ~3 MW of ICRF power for ~1 second

because the radiated power increases throughout the H-mode for the second discharge whereas the radiated power is controlled for the first and progressively worse for following discharges. From these discharges, the estimated erosion rate is 15-20 nm/s. We note that in the original beryllium experiments on JET that significant beryllium influx was observed but the erosion rate was not estimated.[12] Assuming a similar erosion rate for beryllium in ITER as the B erosion rate in C-Mod, the number of discharges to erode through 1 cm of a beryllium is ~1000 discharges (400 second discharges). Thus, any low Z-film or even bulk PFC is likely to have a relatively short lifetime in the presence of RF sheaths.

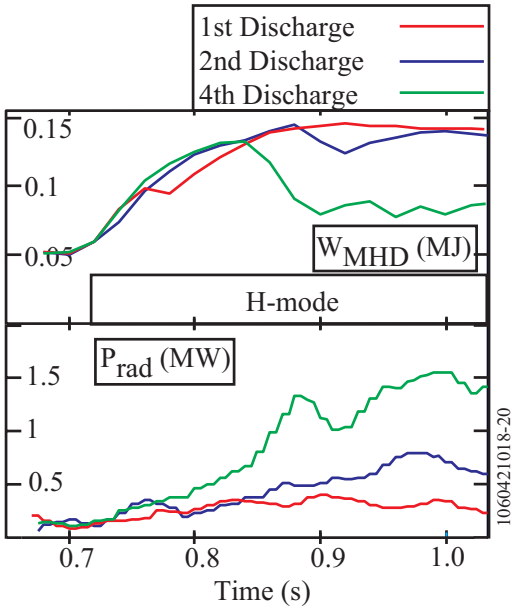


**Figure 1:** Following a boronization, the radiated power during H-modes is controlled for a single discharge heated with 3 MW of ICRF for 1 second. Each of the following discharges has an uncontrolled increase in radiated power.

## 3.0 Measurements of Plasma Potential in presence of ICRF

Since RF sheaths are expected to be important, we sought to characterize the RF sheaths through measurements of the plasma potential using emissive probes. Two emissive probes are utilized to measure the plasma potential on field lines that connect the RF antenna and plasma limiter and are shown schematically in Figure 2. These probes consist of thin thoriated tungsten wire where the emitted electron current is greater than the free streaming electron flux. The floating potential of the heated filament is a measure of the plasma potential to with ~Te.[13] The A-side probe maps to antenna 2 (J antenna) and the B-side probe is linked magnetically to the antenna 1 (D/E antenna) and both probes are linked to regions where the RF sheath is expected to be significant.[14, 15, 16] The local RF limiters at the antennas are ~1 cm radially behind the plasma limiters and can be armored with either molybdenum or boron nitride tiles. Measurements confirmed that the plasma potential responds primarily when the probe is magnetically linked to the active antenna.[10] In the following discussion, all the results correspond to B-side emissive probe which is linked to Antenna 1 due to the larger available data base.

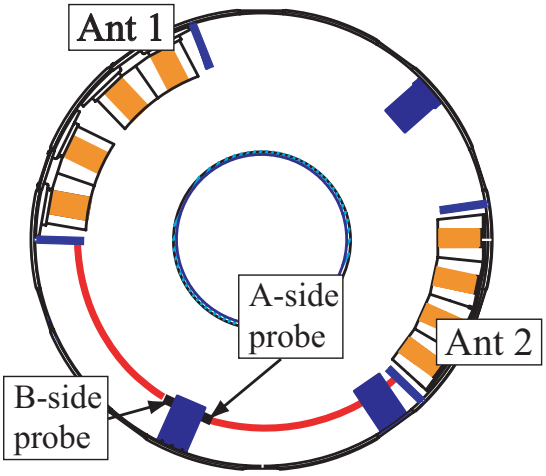


**Figure 2:** The emissive probes are located on a limiter with B-side probe magnetically linked to Ant 1 and A-side probe linked to Ant 2.

In Figure 3, the scaling of the plasma potential with RF power is shown for discharges following a boronization and those without recent boronization. At the highest power level, the plasma potential can be 100-150 V for the latter case while ~60 V just following boronization. Furthermore, the plasma potential scales as the square root of the RF power for the boronized case whereas in the case without recent boronization the voltage scales linearly with power. The sheath voltage is expected to scale with the antenna strap current which can be related to the delivered RF power.[17, 18] There are also differences in RF-induced sheaths between L-mode and H-mode discharges. In Figure 4 we show a comparison of L and H-mode data from separate discharges. Here, the H-mode plasma potentials are higher than the L-mode case by about a factor of 2. Furthermore, the measured plasma potential was essentially the same with BN tiles as with Mo tiles.

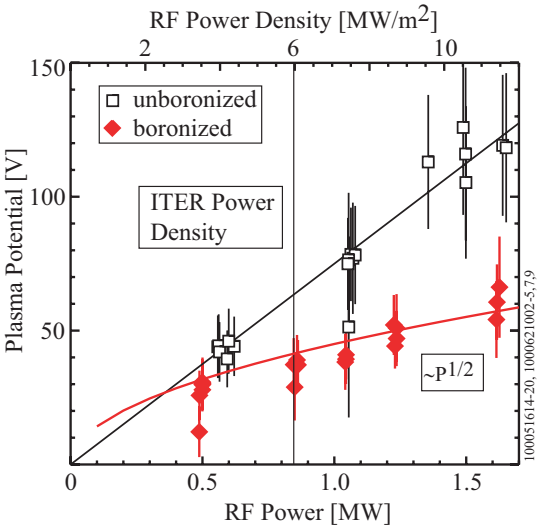


**Figure 3:** In L-mode discharges, the measured plasma potential scales as the square root of the RF power for recently boronized PFCs and linear with RF power for un-boronized PFCs.

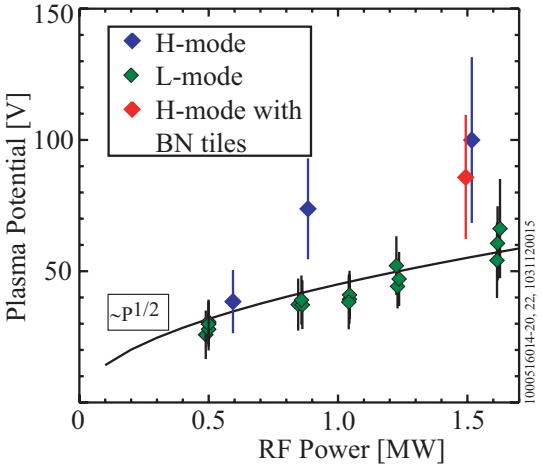


**Figure 4:** Comparison of the measured plasma potential for L and H-mode discharges showing that the H-mode potential is ~2x L-mode. Comparing an H-mode discharge with BN tiles, shows the RF sheath is unaffected relative to the RF sheath in H-mode with metallic RF limiter tiles.

Based on Phaedrus-T experiments [19] and the RF sheath model, we expected that switching the antenna limiter tiles to BN would eliminated the primary Mo source affecting the plasma.[20] However, the C-Mod data clearly indicates the presence of RF sheaths despite thick BN tiles on the RF limiter. One possible explanation is that the RF sheath model needs to allow for cross-field currents.[21, 22] In such a case ion flows across the magnetic field along the length of the flux tube between antenna and main limiters and would be balanced by electron currents in and out of one end of the flux tube still connected to Mo tiles. This would require the impedance integrated along the flux tube to be less than or equal to the impedance through the sheath. Another possibility is the development of an energetic edge electron population. We note that relatively small energetic electron population, ~0.1% can double the sheath voltage and a population of a few percent can increase the sheath potential by a factor of 10.[23] A number of mechanisms have been proposed, two of which are Fermi acceleration[24] and near field acceleration similar to that observed with lower

hybrid couplers.[25] Both mechanisms would create electrons on field lines linked to the active antenna and might not have been dominant in the Phaedrus-T experiment because of the low power, 10-40 times less than C-Mod's, used in those experiments.

The RF sheath model predicts that the RF sheath voltage should scale as the square root of the RF power.[17] For the recently boronized case, the plasma potential follows the predicted trend. However, when the B layer is eroded, the plasma potential scales with the RF power. This suggests that the induced plasma potential can be influenced by factors other than the RF voltage. A possible explanation is that the local density profile is changing with RF power and complicating the scaling. Although direct measure of the density profile is lacking, the antenna load gives an indirect measure of the profile because of the sensitivity to the density profile. In these power ramps, the antenna loading is constant above 100 kW.

Another indication that other factors can influence the RF sheath voltage is the increased RF sheath in H-mode compared to L-mode. If one assumes that the surface conditions were held constant across a transition from L and H-mode, one would expect that the induced sheath voltages would increase with the current in the antenna strap based on the RF sheath model. From current probes in the antenna and measurements of the antenna resistance, the RF sheath voltage was expected to increase by ~20% for the case shown in Figure 4, but the observed RF sheath voltage nearly doubled. This further indicates the RF sheath voltage per applied RF voltage is strongly dependent on other factors. For sake of discussion, assume the RF sheath voltage is set by an edge energetic electron population. In the case of H-mode, the edge collisionality is lower than in L-mode; thus, the electron population can be more energetic and a larger fraction of the total electron population. This would lead to larger RF sheath voltages in the H-mode case compared to the L-mode regime.

## 4.0 Performance of Real Time Matching Network

Plasma load variations are commonly encountered during ICRF heating of fusion plasmas, L to H transitions and edge localized mode activity (ELM's) for example, and present a significant challenge to ICRF utilization for present and future fusion devices. To maintain efficient power transfer, a matching network needs to adjust to the antenna loading variation in real-time or be tolerant to these variations. For ITER, the matching network is a combination of conjugate tee and ELM dump. The system is passive and results is some power being deposited in the ELM dump. The conjugate tee configuration is based upon connecting two identical and independent antenna straps such that the reactive load variations essentially cancel at the input to the conjugate-T resulting in resistive input impedance. We had previously implemented a conjugate tee network on one antenna and found that the coupling between antenna elements was too strong resulting in destruction of load tolerance.[26] We also considered a number of other real time control configurations before pursuing a matching network based upon ferrite tuners but due to various constraints the ferrite tuner approached proved to be more advantageous.[27]

The matching network used in these experiments is a triple stub system where the first stub, closest to the antenna, is fixed and the other two stubs are ferrite tuners and are connected to the E antenna. The ferrite tuners are parallel plate transmission lines loaded with ferrite material and were made by Advanced Ferrite Technologies (specifications can be found in

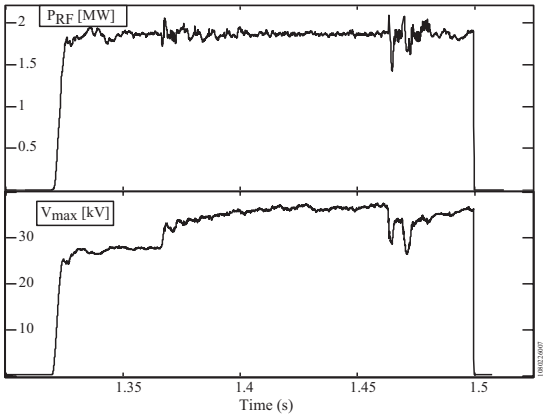


**Figure 5:** RF pulse into plasma with a maximum injected power of 1.85 MW and maximum voltage of 37 kV were obtained for short pulses.

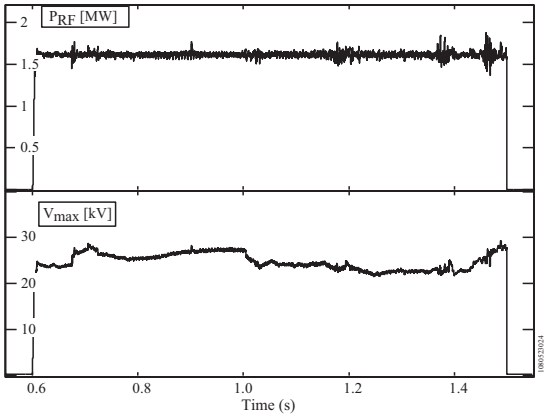


**Figure 6:** As a result of higher loading, high power pulses of 1.6 MW with lower maximum voltage were obtained.

Ref. [28]). To minimize losses, the ferrite tiles are magnetized by a permanent field ~0.016 T. For ferrite material near magnetic saturation ($M_0$), its permeability, $\mu$, varies approximately as $M_0/H$, where H is the strength of applied magnetic field. To change the effective electrical length of the tuner, the bias field can be increased or decreased by a second magnet to modify the effective permeability of the ferrite material. For example, decreasing the bias magnetic field will increase the effective $\mu$ and increase the electrical length of the tuner. The requirement of low loss (i.e., adequate biasing field) sets an upper limit of $\mu$ that a system can change. Each tuner has an electromagnet (24 turns each) above and below the ferrite tiles to generate a bucking field, approximately perpendicular to the ferrite material. The power supply can provide current ranging from -150 A to 150 A where the resulting bucking field is approximately +90 Gauss to -90 Gauss. The electrical length is ~36 cm (~0.1$\lambda$) at 80 MHz. The power supply limits the coil current slew rate to 75 A/ms, corresponding to ~9 cm/ms, and full range to be covered in 4 ms.

Real time matching is achieved by controlling the tuner electrical length, via the current in the electromagnet, in feedback. Directional couplers measure the forward power, reflected power, and phase at four different locations in the transmission line. These signals are used to calculate the local complex voltage reflection coefficient $\Gamma$ and using a model of the network to calculate the required stub lengths to obtain perfect match. The total computation time is 200 $\mu$s and more detailed description of the control system can be found in Ref. [29].

Although a triple-stub configuration can match to any antenna loading in principle, the Alcator C-Mod system is designed to cover a range of the antenna loading corresponding to most of the observed C-Mod L and H-mode antenna loading. The principle characteristics we sought to evaluate are the voltage and power handling, system time response, and losses.

Since the system is a prototype, we sought to characterize the voltage and power limits. Using H-mode and L-mode discharges, we demonstrated the first successful implementation at high power (1.85 MW coupled) into H-mode and low VSWR maintenance over a wide range of plasma conditions. An example is shown in Figure 5 and a 1 second, 1.6 MW RF pulse is shown in Figure 6. The pulse length and power limits appear to be at least as long as

the typical C-Mod plasma discharge duration (~1.5 s current flat top). The maximum voltage achieved in the unmatched section of the matching network reached 37 kV. We found that one of the tuners had a lower maximum voltage by ~25% lower than other and was arcing near the transition from coax to parallel plate transmission line.

In Figure 7, the plasma has an L to H-mode transition at 0.65 sec and evolves over the course of the discharge. The antenna loading also evolves and the matching network follows these load changes well as evident by the less than 10 kW out of 1 MW reflected. The coil currents on the tuners are shown in third panel. At the L-H transition, the reflected power rose because of the sudden loading change, but the feedback system was able to reduce it to below 1% in less than 600 μs, and the reflected power only rose to a maximum at 40 kW (4%) at the transition. If the tuner currents were fixed, the reflected power would have reached approximately 150 kW. The FFT system has been demonstrated to maintain the matching in almost all plasmas in C-Mod (Ip from 0.4 to 1.2 MA and line-averaged density from 0.5 to $3x10^{20}$ $m^{-3}$), including the special cases such as during the current ramp-up and deuterium pellet injection.

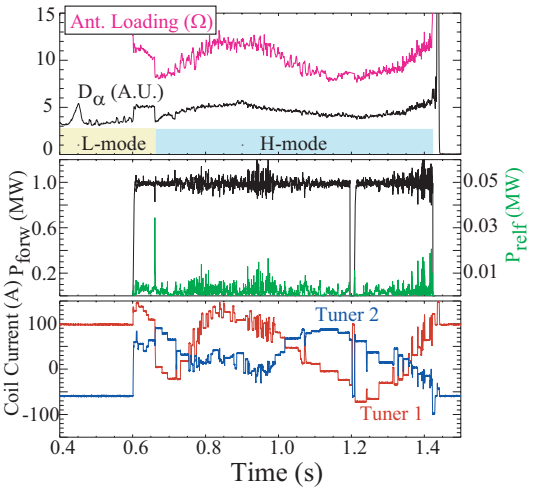


**Figure 7:** Example discharge showing the matching network maintaining low reflected power despite significant load variations. The first panel shows the antenna loading and Dα signal. The second panel shows the forward and reflected RF power and the third panel shows the coil currents.

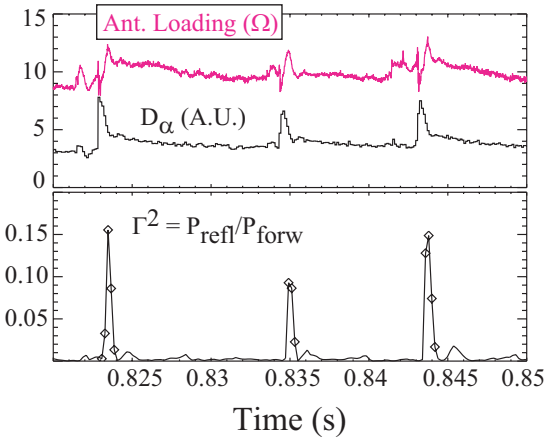


**Figure 8:** Time response of the matching network is sufficient to limit the reflected power during an ELM but not match it throughout the event.

The speed of this FFT system is not optimal for plasmas with ELMs, but limits the matching excursion associated with the ELM. A typical ELM on C-Mod plasmas has rise time about ~50-100 μs, while the FFT system adjusts its matching once per computation iteration (200 μs). In Figure 8, the antenna loading response for large ELMs is shown where the ELM is apparent in the fast rise and decay in the $D_\alpha$ signal and the antenna loading. The power reflection rises to about 10% to 15% but is restored to <1% in ~400 μs where this response is largely set by the computation time. It is unclear at this time whether the ferrite material itself can be fast enough to respond the rise of ELMs.

A principle concern regarding ferrite tuners is excessive power dissipation. Two loss mechanisms are of particular interest, so-called "dynamic loss" and "high loss effect."[30] Dynamic loss occurs when the magnetization is low that occur at low values of bias field and

is present at all RF power levels. The high loss effect occurs at high RF power and at any bias field. For circulating power levels below 4 MW typical of the triple stub configuration, there was no observable significant power loss in the tuners. At higher circulating power levels, we did observe increased power loss but this was also when the bias field was lowest.

**5.0 Acknowledgements**

This work is support by Department of Energy Coop. Agreement DE-FC02-99ER54512.

**References**

[1 ] ITER Physics Expert Group on Energetic Particles, Heating, and Current Drive, Nucl. Fus. **39**, 2495 (1999).
[2] F. Najmabadi and the ARIES Team, Fusion Eng. and Design **80**, 3 (2006).
[3] J. Myra in 16th Top. Conf. on RF Power in Plasmas, AIP Conference Proceedings **787** (2006) 3 and J. Myra et al., Nuclear Fusion **46**, S455 (2006).
[4] J. Jacquinot et al., Fusion Eng Design **12**, 245 (1990).
[5] R.I. Pinsker, Plasma Phys. Control. Fusion **40** (1998), A215.
[6] I.H. Hutchinson, R. Boivin, F. Bombarda et al., Phys. Plasmas **1** (1994) 1511.
[7] Y. Takase et al., 14th Symp. on Fusion Eng., San Diego, 1992, (IEEE, Piscataway, NJ, 1992), p. 118.
[8] S.J. Wukitch et al., Plasma Phys. Control. Fusion **46**, (2004) 1479.
9 B. Lipschultz et al., Phys. Plasmas **13**, 056117 (2006).
10 B. Lipschultz et al., Nuclear Fusion **41**, 585 (2001).
11 S.J. Wukitch et al., J. Nucl. Mater. **363–365**, 491 (2007).
12 M. Bures et al., Fusion Eng. Design **12**, 251 (1990).
13 E. Y. Wang et al., J. Applied Physics **61**, 4786 (1987).
14 D.A. D'Ippolito et al., Nuclear Fusion **38**, 1543 (1998).
15 D.A. Diebold et al., Nuclear Fusion **32**, 2040 (1992).
16 L. Colas et al., Plasma Phys. Control Fusion **49**, B35 (2007).
17 J. R. Myra et al., Fus Eng. Design **31**, 291 (1996).
18 D.A. D'Ippolito et al., Nuclear Fusion **38**, 1543 (1998).
19 J. Sorensen et al., Nuclear Fusion **33**, 915 (1993) and J. Sorensen et al., Nuclear Fusion **36**, 173 (1996).
20 J.R. Myra et al., J. Nucl. Mater. **249**, 190 (1997).
21 D.A. D"Ippolito et al., Nuclear Fusion **42**, 1357 (2002).
22 E. Faudot et al., Phys. Plasmas **13**, 042512 (2006).
23 D. Tskhakaya et al., Phys. Plasmas **9**, 2486 (2002).
24 M. D. Carter, D. B. Batchelor, and E. F. Jaeger, Phys. Fluid B **4**, 1081 (1992).
25 V. Petržílka et al., in Proc. 32nd EPS Conference on Plasma Phys. **29C**, P-2.095 (2005).
26 A. Parisot et al., 31st EPS Conference on Plasma Physics (ECA), **28G**, P-2.168 (2004).
27 Y. Lin et al., "Real-time Fast Ferrite ICRF Tuning System on the Alcator C-Mod Tokamak", accepted by Fusion Eng. and Design.
28 S. Martin, W. Arnold, E. Pivit, AIP Conference Proceedings **244**, 318 (1992).
29 Y. Lin et al, Fusion Eng. Design **83**, 241 (2008).
30 J. E. Griffin and G. Nicholls, IEEE Trans. on Nucl. Sci. **NS-26**, 3965 (1979).